

On glassy behavior in ferroics

Invited Article

Turab Lookman^{*1}, Dezhen Xue¹, Romain Vasseur², Hongxiang Zong^{1,3}, and Xiangdong Ding³

¹Theoretical Division, Los Alamos National Laboratory, Los Alamos, New Mexico 87544, USA

²Institut de Physique Théorique, CEA Saclay, 91191 Gif Sur Yvette, France

³State Key Laboratory for Mechanical Behavior of Materials, Xi'an Jiaotong University, Xi'an 710049, P.R. China

Received 16 December 2013, revised 24 February 2014, accepted 3 March 2014

Published online 11 April 2014

Keywords cooperative behavior, ferroic glass, martensites, perovskites

*Corresponding author: e-mail txl@lanl.gov, Phone: 505-665-0419, Fax: 505-665-4063

Ferroics include a range of materials classes with functionalities such as magnetism, polarization, and strain. We review coexistence and glassy behavior, as studied over the last decade,

in systems such as perovskite manganites, ferroelectrics, and martensites to distill a common theme that includes the interplay of long-range interactions, disorder, and cooperative behavior.

© 2014 WILEY-VCH Verlag GmbH & Co. KGaA, Weinheim

1 Introduction It is well known that a system of strongly interacting, largely via elastic strain fields, phase separated regions undergoes a “dynamic” to a “static” transition reflected in several functional degrees of freedom such as magnetism, lattice, charge, or polarization [1–3]. In analogy with the slow kinetics, relative to the Arrhenius law, observed in glass-forming matter comprised of atoms, molecules, polymers, etc., we have started to refer to materials undergoing such behavior as *ferroic glasses*. In structural glasses the deviations from thermal activation arise from the increase in cooperative behavior of the molecular constituents when approaching the glass transition [4]. Atomistic simulations are beginning to give us clues on the nature of the cooperativity (e.g., “string” like motions in the freezing of a fluid at the glass transition) and the growth of the correlation length scales. Recently, experiments have started to probe this self-organization in glass forming liquids, such as glycerol via nonlinear susceptibility measurements, which are related to higher-order correlation functions that encode aspects of the cooperative behavior [4]. Such experiments show that the number of correlated molecules or elements grows rapidly as the glass transition is approached. A comparable level of measurements and understanding in ferroic glasses, especially on aspects related to the nature of the cooperative behavior, is so far lacking. Thus, one of the challenges in the field is to move beyond simplified notions of “frozen” defects or states involving spins, dipoles or martensite variants in a matrix, in terms of which we are accustomed to thinking because of spin glass-like ideas, to probing cooperative, structural organization which appears at

the heart of understanding glassy behavior in a wide class of materials. Our purpose here is to review and relate ideas that span glass physics: from structural glasses and gels and colloids to manganites, ferroelectrics and martensites, and distill a common theme to suggest that glassiness in martensites is likely related to a form of cooperative behavior.

2 Perovskite manganites The importance of long-range strain fields in mediating glassy physics in ferroics has been well recognized in the perovskite manganites where the interplay between spin, charge, and the lattice gives rise to coexisting regions of insulating, charge-ordered (CO) and metallic, ferromagnetic (FM) phases [1–3, 5]. The phase diagram for the perovskite manganese oxide, $\text{La}_{0.215}\text{Pr}_{0.41}\text{Ca}_{3/8}\text{MnO}_3$ (LPCMO), obtained in Ref. [1] is shown in Fig. 1. A CO phase leads to a coexistence of CO/FM domains that can be up to micron size, which on further cooling give rise to a glass state. The phase boundaries were determined by resistivity, magnetization, and resonant ultrasound measurements and the onset of the glass transition was also characterized by deviation of the zero-field-cooled magnetization and susceptibility from the field-cooled result. The authors of Ref. [1] introduced the term/concept of a “*strain liquid*” for the CO/FM phase to signify its dynamic, fluctuating character and “*strain glass*” for the kinetically frozen, static glass phase below the glass transition. The transition is a freezing of large fluctuations in resistivity, magnetism and internal friction from a dynamic to a static phase where there is a marked drop in magnetic relaxation. Whether the glass phase is a cluster glass in which

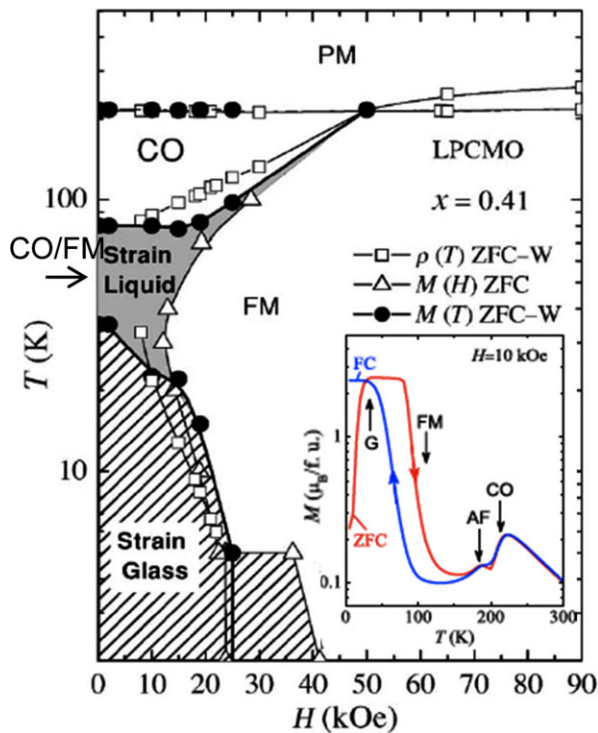


Figure 1 Phase diagram for $\text{La}_{0.215}\text{Pr}_{0.41}\text{Ca}_{3/8}\text{MnO}_3$ reproduced from Ref. [1] showing phases (CO, charge ordered; FM, ferromagnetic metallic) and their coexistence. There is a transition characterized by a freezing from a “dynamic” phase with large fluctuations in resistivity, magnetism, and internal friction to a “static” glass phase. Inset from Ref. [2] shows signature of magnetic irreversibility such as the reduced magnetism in ZFC/FC curves.

magnetization clusters in the CO matrix essentially freeze as individual spins below the glass transition, is an interesting question. This is what is expected to occur in magnetic alloys such as CuMn. However, such spin glass-like behavior has also been observed in many colossal magnetoresistance (CMR) materials with the assumption that the magnetic domains or clusters behave as in cluster glasses. We now know that this picture is not accurate. Rather, the volume fraction of FM clusters substantially decreases in the glass state. In the case of a spin or cluster glass individual spins or clusters are frustrated in their orientation without exhibiting any long-range order. Here, in addition to that possible freezing, there is the magnetic relaxation due to the change in FM volume fraction, and as this magnetic relaxation drops, the phase separation is dynamic above and static below the glass transition temperature. Since the coexistence of CO/FM involves interfaces between orthorhombic and pseudocubic distortions, results on dissipation from resonant ultrasound measurements indicate that these interfaces are highly fluctuating in the strain liquid region and become kinetically hindered below a glass transition. The overall geometrical morphology of these interfaces is an interesting question. The development of novel high-resolution spectroscopies are beginning to throw light on the details

of the metal-insulator transition. For example, “stripe-like” domains have been imaged recently in VO_2 [6] that are not pinned by defects so that their spatial arrangement can fluctuate. This suggests a form of cooperative behavior. The role of chemical randomness competing with electronic phase separation has also been discussed in detail [7] with the use of models based on the random field Ising model (RFIM). However, such approaches do not capture the elastic interactions appropriately. In addition, the inhomogeneous features generated from such modified RFIMs are the result of assuming that the metallic and insulating states (modeled as spin up and down states) have exactly the same energy in the average field, which is an inadequate assumption for the inhomogeneity in manganites due to the lack of symmetry between metallic and insulating states. It has been shown that the correction to this in the modified RFIM leads to a homogeneous phase [8]. A number of studies over the last decade have also emphasized the role of martensitic-like accommodation in inducing long-range strain interactions and giving rise to inhomogeneity and intrinsic self-organization (without the need to add disorder) that result in CMR effects and glassy morphologies [5]. These include Landau-like descriptions for nanoscale texturing with coupled functionalities [9]. We therefore next consider the origin of glassy behavior in martensitic alloys where strains/shuffles act as order parameters. This allows us to isolate competing aspects such as the influence of the long-range elastic interaction and the degree of doping or disorder, without additional functionalities or fields.

3 Martensite glass There has been renewed interest in understanding the slow kinetics and glass-like behavior in martensitic and shape memory alloys. Recent experiments on ferroelastic alloys have shown that by introducing disorder by doping above a critical value an abnormal glass-like state, interpreted as a frozen state of local strain order, can be generated below a transition temperature [10, 11]. This so called “strain glass,” perhaps better termed “*martensite glass*” in this case, is of interest not only from a theoretical perspective but it has been shown to display superelasticity and shape memory effects, which are typically seen in austenite and martensite [12, 13]. However, the nature of the glass behavior, in terms of its relationship to the glass physics seen in other ferroics or structural materials, is far from clear. As for the perovskite manganites, the experimental diagnostics have largely relied on signatures for ergodicity breaking, such as FC-ZFC behavior and frequency dispersion of dynamic properties. Structural analysis via high-resolution electron microscopy (HREM) has so far not been refined enough to test hypotheses. Theoretically, the tweed phase was the subject of several early studies that interpreted and mapped it as a spin glass phase [14]. However, experiments on alloys such as $\text{Ti}_{50}\text{Ni}_{47}\text{Fe}_3$ have shown no frequency dispersion or changes in moduli in the premartensitic tweed regime [11, 15]. Care needs to be exercised in using diagnostics such as ZFC/FC magnetization or the frequency dependence of the AC

susceptibility as similar signatures of glass behavior can be seen in mechanically alloyed ferromagnetics such as $\text{Fe}_{61}\text{Re}_{30}\text{Cr}_9$ [16]. Even $\text{Ti}_{50}\text{Ni}_{47}\text{Fe}_3$ shows deviation between the ZFC/FC curves that gets greater at temperature $T < A_s$, the austenite start temperature. This is interpreted as a signature for breakdown of ergodicity but this is a normal martensite and not a glass at low temperatures.

3.1 Models Although the importance of the elastic long-range interaction and disorder via chemical inhomogeneity or compositional fluctuations was well recognized in the context of manganites, ferroelectrics and martensites, recent experiments on martensite glass have generated a number of studies attempting to predict the glass state. These essentially are of two types: (i) those that solve a relaxation dynamics equation based on a continuum Landau free energy approach and include elastic energy terms and added disorder [17, 18], and (ii) those that map the continuum Landau description into a discrete model so that the tools of statistical mechanics that have been used to study spin glass behavior, may be readily employed [19–22]. Our focus here will be on approach (ii) as it provides predictive results because an order parameter that identifies the glass phase can be defined and mean-field theory and renormalization group approaches can be utilized to predict it. Simulations probing glass behavior often require special consideration and these have been developed to a greater degree using Monte Carlo methods applied to discrete models. We consider for simplicity the 2D square to rectangle transformation driven by the deviatoric shear (see Fig. 2) which serves as an order parameter. This transition is a 2D analog of a cubic to tetragonal or tetragonal to orthorhombic transformation and is one of the simplest that illustrates the salient physics. The strains are defined in terms of the lattice displacements, u , by Eq. (1):

$$\varepsilon_{ij} = \frac{\partial u_i / \partial r_j + \partial u_j / \partial r_i}{2}, \quad (1)$$

from which the strain tensor components, ε_{xx} the longitudinal strain, ε_{yy} , the transverse strain and the simple shear strain, ε_{xy} , as well as their symmetrized components e_1, e_2, e_3 are

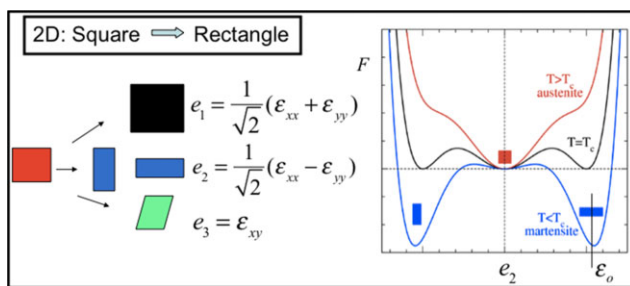


Figure 2 Principal strain modes for square with e_2 as the order parameter (OP) for the square to rectangle transformation. Free energy curves as a function of temperature showing the first order transition at temperature T_c .

defined. As there are only two displacements in 2D, the three strain components are related through the compatibility condition,

$$(\partial_{xx} + \partial_{yy})e_1 - (\partial_{xx} - \partial_{yy})e_2 - \sqrt{8}\partial_{xy}e_3 = 0, \quad (2)$$

being derivatives of the same underlying displacement field. From a computational point, a key difference between our approach [19] and that typically used in the phase field approach is that we eliminate the displacements using equation (2), as distinct from satisfying mechanical equilibrium and solving for the displacements [22]. Figure 2 and the left panel of Fig. 3 show the essential model with a free energy for a first-order transition so that at high temperature there is minimum corresponding to the austenite phase and below the martensitic transition temperature, T_c , there are two minima corresponding to the two martensite variants or homogeneous states. At the transition the minima are degenerate in energy. Variations in the order parameter (OP) strain are incorporated in a gradient term which is zero in the homogenous or bulk variants and its strength is related to the energy cost of creating interfaces between variants. It is commonly assumed that this term, which controls the width of domain walls between variants, is phenomenologically added. However, this can be derived systematically by considering strain and short wavelength distortion modes which become important as one probes the discreteness of the lattice at nanoscales [5]. Finally, the anisotropic long-range repulsive interaction between the OP strains in 2D is a consequence of eliminating the displacements in the compression-shear energy. This model and its variations have been applied to study how intrinsic inhomogeneities arise, including when coupled to magnetization and charge [9], and the continuum descriptions have been very successful in elucidating and simulating microstructure evolution. Disorder has also been added to affect the transition temperatures and drive the system to a martensite glass [17, 18]. In these studies the glass behavior is monitored largely by the deviation in ZFC/FC curves (as in experiment) and/or “glass like” morphology. The difficulty with this is that it is not so straightforward to identify a glass. Thus, the models tend not to be particularly predictive as none of these studies attempt to evaluate a glass or spin-glass OP.

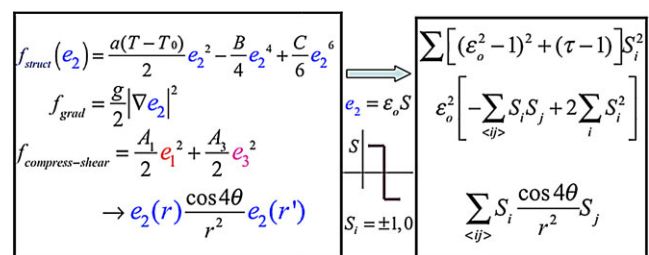


Figure 3 Mapping from a continuum Landau model for square to rectangle transformation to a discrete, “pseudo” spin model when strain e_2 is replaced by discrete “spin” values, $S = 0, \pm 1$.

3.2 Glassy behavior using a discrete model An alternative, yet complementary approach is to formulate a discrete “pseudo spin” model for martensites to which we can add quenched disorder of varying strengths and use the methods of statistical mechanics to allow us to identify and distinguish the different phases [19]. For example, the Renormalization Group (RG) approach integrates out microscopic degrees of freedom so that the attractive basins characterize the physics at large scales. The values of the interaction strength and strength of disorder uniquely characterize the different phases, including the glassy state, thereby allowing the phase diagram in terms of temperature and disorder to be predicted. If we replace the OP strain, e_2 , for the square to rectangle transformation by the discrete variable, S , using $e_2 \rightarrow |e_2|S$, where $S = 0, +1, -1$ tracks the minima of the free energy representing austenite and the two martensite variants, then the nonlinear Landau free energy (right panel Fig. 2) collapses to the linear crystal-field form $w(T)S^2$ as $S^2 = S^4 = S^6$, where the coefficient, w , is some function of temperature. Similarly, the gradient or interaction energy term $\frac{g}{2}|\nabla e_2|^2$ may be written in terms of the product $S_i S_j$ involving discrete S values on neighboring sites $\langle i, j \rangle$ by using the finite difference definition of gradient. Thus, the energy of the original square to rectangle problem (Fig. 3) now transforms to

$$H = - \sum_{\langle i, j \rangle} J_{ij}(T) S_i S_j + w(T) \sum_i S_i^2 + A_1 \sum_{ij} S_i U_{ij} S_j,$$

with $S_i = 0, \pm 1$, and where U is the long-range anisotropic elastic interaction with strength A_1 . This is the well known spin-1 model with long-range interactions [21, 22]. The constant J is related to the interface energy, g , and the minimum energy configuration or ground state of H gives the characteristic twin microstructure in 2D and 3D for a cubic to tetragonal transformation [24]. Such models, despite their simplicity, capture the salient physics of the continuum description and have the advantage of being amenable to study by methods used for spin glasses. However, such a model is an effective model that can predict generic,

universal features, such as the topology of the phase diagram rather than quantitative comparisons to experiments.

In analogy with usual spin glasses for ferromagnetics, we can add disorder to mimic the effects of changing composition in the alloys or fluctuations. Starting from the above disorder-free Hamiltonian, without the long-range interaction, we take the nearest neighbor couplings to be quenched independent random variables J_{ij} drawn from the distribution $P(J_{ij})$ with mean $J(T)$ and variance, σ_J that is a measure of the quenched disorder in the system. The form of the distribution is quite irrelevant to the topology of the phase diagram, which emphasizes that our approach is an attempt to distill salient, universal features. The phase diagram obtained by using a real-space RG approach is shown in Fig. 4a. We have found this approach to be simpler and more reliable than the replica/mean-field approach for this model because in addition to the glass phase, it does predict a tweed precursor phase, consistent with our Monte Carlo simulations. The martensite (ferroelastic) phase corresponds to the usual ordered ferromagnetic phase and in terms of order parameters (OPs) used in mean field theory and replica calculations (see e.g., Ref [22]), this phase is characterized by a non-zero magnetization $m = \langle S_i \rangle \neq 0$, where the bar represents average over the disorder and the brackets average with respect to Boltzmann weights. We find two paraelastic disordered phases with one favoring $S = 0$, and the other interpreted as tweed with the OP “martensite volume fraction” $p = \langle S_i^2 \rangle$ that allows to distinguish between both phases. We find the tweed precursor to be ergodic and non-glassy, consistent with recent experiments [15]. The last phase corresponds to a spin/strain glass with “infinite randomness.” The effective Hamiltonian describing the system at large scales has favors variants $S = \pm 1$ and this phase is also characterized by the Edward–Anderson order parameter $q = \langle S_i^2 \rangle$ which in the replica language corresponds to the overlap between two replicas $q = \langle S_i^1 S_i^2 \rangle$ of the system. In the absence of disorder ($\sigma_J = 0$), we find a first order phase transition between the austenite and martensite phase with $\tau \approx 1$, as expected. As one increases the disorder, an intermediate tweed phase

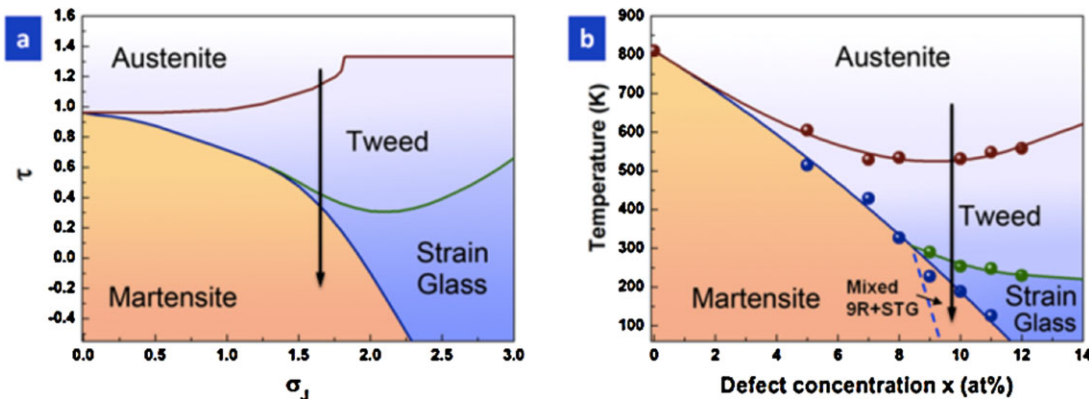


Figure 4 The predicted phase diagram (normalized temperature vs. strength of disorder) from the discrete model compared to that for $\text{Ti}_{50}\text{Pd}_{50-x}\text{Cr}_x$ [19]. The arrow indicates the formation of martensite from the glass phase.

arises before it transforms into a low temperature phase (either martensite or glass). For large enough disorder and low temperature, we find a spin glass phase that we interpret as martensite glass. Interestingly, when the disorder of the system is in the intermediate regime ($1.3 < \sigma_J < 2.3$ in our model), we predict a spontaneous phase transition from glass to martensite for a given concentration. This has been confirmed in studies on the phase transformation behavior as function of temperature T and concentration x for $\text{Ti}_{50}(\text{Pd}_{50-x}\text{Cr}_x)$ alloys (Fig. 4b). For low Cr-concentrations ($x < 8$), the system undergoes a B2 \rightarrow B19 martensitic transformation. For high Cr-concentrations ($x > 12$), the glass transition takes place. For the crossover regime ($9 < x < 12$) between martensite and glass, the alloys experience the parent phase, tweed, glass as well as martensite upon cooling and the spontaneous transformation from the glass to martensite (9R) takes place.

3.3 Interplay between long-range elastic interaction and disorder The analytical phase diagram obtained above does not include the long-range interaction and does emphasize that disorder in the interactions is enough to capture the salient features in the experimental phase diagram shown in Fig. 4. However, Monte Carlo simulations in the presence of the long-range interactions, although not predictive, do provide a consistency check. Figure 5(1a)–(1d) shows typical microstructures obtained in different regions of the phase diagram on a 256×256 lattice, with the strength of the long-range term of $A_1 = 4$. These textures are fully consistent with what is observed in continuum GL theories and in experiments. In particular, we find the usual cross-hatched pattern for the tweed phase. Nevertheless, our RG approach provides a clear meaning to the tweed phase, even in the absence of long-range interactions. We also show in Fig. 5(2) FC/ZFC curves that are usually used in both numerical studies and experiments to test for breaking of ergodicity and glassiness. These curves were obtained by averaging over 1000 disordered configurations on 64×64 lattices, other lattice sizes were tested without much

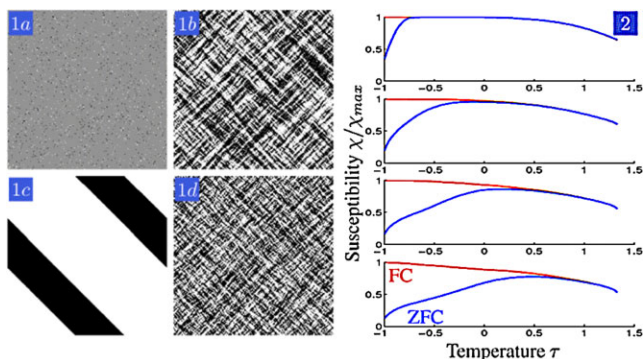


Figure 5 (1a–1d) Typical microstructures obtained in different regions of the phase diagram on a 256×256 lattice, with the strength of the long-range term of $A_1 = 4$. (2) FC and ZFC curves for testing the breaking of ergodicity and glassiness, obtained by averaging over 1000 disordered configurations on 64×64 lattices.

difference. The curves shown in Fig. 5(2) may be interpreted as a signature of history dependence or ergodicity breaking. There are subtle issues of whether the 2D version of the Hamiltonian strictly has a spin-glass phase, these are discussed in [19]. Finally, the main features of our phase diagram in Fig. 4 persist even in the presence of the long-range interactions. The competition between the elastic long-range interaction and disorder on the austenite/tweed and tweed/glass transition temperatures is shown schematically in Fig. 6. For no disorder ($\sigma_J = 0$), the austenite/martensite transition temperature is shifted to lower temperatures with increasing A_1 . Figure 6 has implications in the study of colossal magneto-resistance (CMR) materials where the interplay of disorder and long-range strain mediated interactions has a bearing on phase separation of coexisting insulating and conducting phases.

As discussed in Section 2, the effects of quenched disorder have been studied in manganites, where a first-order transition separates the charge-ordered and the competing ferromagnetic phase [7]. Monte Carlo simulations on the RFIM show that as the strength of the disorder increases, a glass phase appears with nanoscale inhomogeneities. These results may not be too surprising as the strain-based spin model for a first-order structural transition presented here has a glass phase with increasing strength of disorder. It would therefore be very interesting to explore and predict the effects of competing interactions and OPs (i.e., magnetism and strain) in the presence of disorder, within the context of the discrete model as compared to the continuum disorder ($\sigma_J = 0$), the austenite/martensite transition temperature decreases linearly with A_1 , as included phenomenologically within Landau theory. All the transition temperatures decrease with A_1 , in particular the glass transition is shifted to lower temperatures because the long-range interactions

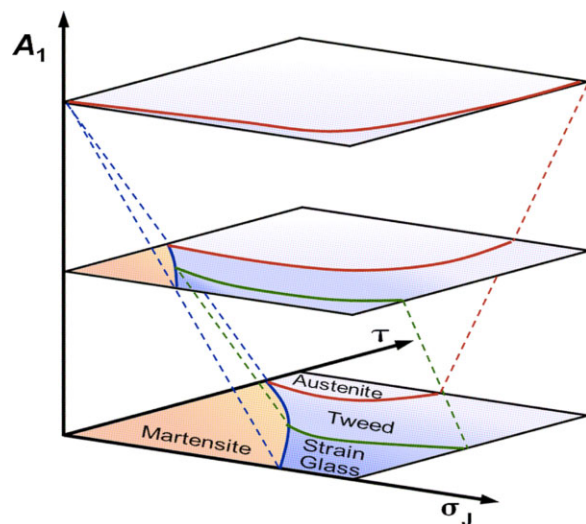


Figure 6 “Phase diagram” with normalized temperature (τ) emphasizing the interplay of the strength of the elastic long-range interaction (A_1) and strength of disorder (σ_J). The long-range interaction shifts the glass transition to lower temperatures [19].

compete with the randomness. In the asymptotic limit $A_1 \rightarrow \infty$, the disorder becomes irrelevant and only the austenite phase remains; we therefore conjecture that the phase diagram is [25].

4 Relaxor ferroelectrics and martensites as network glasses

The behavior of relaxor ferroelectrics has been traditionally construed as the appearance of polar regions in a non-polar matrix at the Burns temperature [26]. These regions or clusters can increase in size on further cooling until the system begins to kinetically freeze where it displays Vogel–Fulcher behavior. This so-called random field (RF) scenario [27–30] invokes quenched random fields that act to create the polar domains. The RFIM, that we have already discussed in connection with manganites, and which has already been used for martensites [20–22], serves as the theoretical lynchpin for this scenario, which certain experiments lend support to [29, 30]. The other scenario involves the notion of cooperative interactions between polar regions that are responsible for the increasing deviation from Curie–Weiss behavior at lower temperatures [31]. This “clustering” scenario (also referred/related to dipolar glass [32]) has been further developed recently in a *network* description from suggestions from experiments and simulations [33]. This considers the relaxor transition to be accompanied by anisotropic nanoscale correlations of the in-phase cation motions. The correlations (via the associated displacements) form a network, analogous to the network of highly anisotropic hydrogen bonds in water. There is thus a network of dipoles that acquires unique properties accompanied by extremely slow relaxation. This is a departure from the concept of localized polar clusters in an inert matrix, as well as finite clusters, as these clusters can become larger and percolate. Similar cooperative behavior is seen in glass formers, such as glycerol and propylene carbonate as the glass transition is approached [4]. Here the number of correlated molecules increases and is the cause of the slowing down and departure from Arrhenius behavior in the vicinity of the transition. However, in the case of relaxors there is clearly a need for high-resolution spectroscopy measurements to directly probe network features.

The current, prevalent picture of martensite glass that we have described in Section 3 is that of kinetically frozen localized variants in a matrix of the parent phase, and the models utilize the elastic long-range and disorder to capture aspects of the phase diagram and non-ergodic behavior. However, in analogy with the scenario described above for ferroelectric relaxors, it is tantalizing to speculate whether martensite glass can show similar cooperative, *network-like* behavior. Our unpublished theoretical and experimental work suggest a network of strain correlations in the glass phase that determine its properties, as distinct from that of the matrix [34]. This picture is appealing as it is also consistent with glassy behavior due to network formation in glass formers, colloidal glasses and phase separating amorphous alloys such as $\text{Cu}_{50}\text{Nb}_{50}$ [35], where the glass

transition is accompanied by the formation of a mechanically stiff, percolating network.

An even broader question relates to the description of the glassy state itself in terms of whether the domain/droplet model [36], in contrast to the free energy landscape hierarchical model [37], is appropriate for ferroics in the glass state. Rejuvenation and memory experiments on spin glasses have previously suggested a hierarchical picture [38] of a free energy landscape where the metastable minima split into further minima as the temperature is lowered. More recent experiments on rejuvenation and memory in spin glasses show a symmetrical response on cooling as well as on heating [39]. The situation for relaxors is also not completely clear with several studies favoring the hierarchical picture valid only for the cooling protocol [40] and others showing symmetric behavior irrespective of heating or cooling [41]. Such rejuvenation and memory experiments for martensite alloys, which we are currently undertaking, will aid in unlocking the nature of its glassy state.

5 Summary We have attempted to distil the role of the long-range elastic interaction and disorder in determining glass-like behavior in ferroics that include perovskite manganites, martensites, and ferroelectrics. The role of cooperative behavior and correlations has been well studied in structural glasses and has been emphasized in perovskite manganites and in relaxor ferroelectrics. How these latter ideas relate to the problem of martensite glass, or other ferroics such as magnetoelectrics, is an interesting question for further study.

References

- [1] P. A. Sharma, S. B. Kim, T. Y. Koo, S. Guha, and S.-W. Cheong, *Phys. Rev. B* **71**, 224416 (2005).
- [2] P. A. Sharma, S. El-Khatib, I. Mihut, J. B. Betts, A. Migliori, S. B. Kim, S. Guha, and S. W. Cheong, *Phys. Rev. B* **78**, 134205 (2008).
- [3] W. Wu, C. Israel, N. Hur, S. Park, S.-W. Cheong, and A. De Lozanne, *Nature Mater.* **5**, 881 (2006).
- [4] Th. Bauer, P. Lunkenheimer, and A. Loidl, *Phys. Rev. Lett.* **111**, 225702 (2013).
- [5] K. H. Ahn, T. Lookman, and A. R. Bishop, *Nature (London)* **428**, 401 (2004).
- [6] M. K. Liu et al. *Phys. Rev. Lett.* **111**, 096602 (2013).
- [7] A. Moreo, S. Yunoki, and E. Dagotto, *Science* **283**, 2034 (1999).
- [8] K. H. Ahn and T. Lookman, arXiv: cond-mat/0408077 (2004).
- [9] A. R. Bishop, T. Lookman, A. Saxena, and S. R. Shenoy, *Europhys. Lett.* **63**, 289 (2003).
- [10] S. Sarkar, X. Ren, and K. Otsuka, *Phys. Rev. Lett.* **95**, 205702 (2005).
- [11] X. Ren et al. *Philos. Mag.* **90**, 141–157 (2010).
- [12] Y. Zhou, D. Xue, X. Ding, K. Otsuka, J. Sun, and X. Ren, *Appl. Phys. Lett.* **95**, 151906 (2009).
- [13] Y. Wang, X. Ren, and K. Otsuka, *Phys. Rev. Lett.* **97**, 225703 (2006).
- [14] S. Kartha, T. Castàn, J. A. Krumhansl, and J. P. Sethna, *Phys. Rev. Lett.* **67**, 3630 (1991).

- [15] Y. Murakami, H. Shibuya, and D. Shindo, *J. Microsc.* **203**, 22 (2001).
- [16] J. A. De Toro, M. A. L. de la Torre, M. A. Arranz, J. M. Riveiro, and J. L. Martinez, *J. Appl. Phys.* **87**, 6534 (2000).
- [17] P. Lloveras, T. Castán, M. Porta, A. Planes, and A. Saxena, *Phys. Rev. B* **80**, 054107 (2009).
- [18] D. Wang, Y. Wang, Z. Zhang, and X. Ren, *Phys. Rev. Lett.* **105**, 205702 (2010).
- [19] R. Vasseur, D. Xue, Y. Zhou, W. Ettoumi, X. Ding, X. Ren, and T. Lookman, *Phys. Rev. B* **86**, 184103 (2012).
- [20] D. Sherrington, *J. Phys.: Condens. Matter* **20**, 304213 (2008).
- [21] S. R. Shenoy and T. Lookman, *Phys. Rev. B* **78**, 144103 (2008).
- [22] R. Vasseur and T. Lookman, *Phys. Rev. B* **81**, 094107, (2010).
- [23] M. Porta and T. Lookman, *Acta Mater.* **61**, 5311–5340 (2013).
- [24] R. Vasseur, T. Lookman, and S. R. Shenoy, *Phys. Rev. B* **82**, 094118 (2010).
- [25] P. Lloveras, G. Touchagues, T. Castán, T. Lookman, M. Porta, A. Saxena, and A. Planes, *Phys. Status Solidi B* **251**, 2080–2087 (2014), this issue.
- [26] L. E. Cross, *Ferroelectrics* **76**, 241 (1987).
- [27] W. Kleemann, et al. *Appl. Phys. Lett.* **102**, 232907 (2013).
- [28] V. Westphal, W. Kleemann, and M. D. Glinchuk, *Phys. Rev. Lett.* **68**, 847 (1992).
- [29] A. K. Tagantsev and A. E. Glazounov, *Phys. Rev. B* **57**, 18 (1998).
- [30] D. Fu, H. Taniguchi, M. Itoh, S. Koshihara, N. Yamamoto, and S. Mori, *Phys. Rev. Lett.* **103**, 207601 (2009).
- [31] D. Viehland, S. J. Jang, L. E. Cross, and M. Wuttig, *Phys. Rev. B* **46**, 8003 (1992).
- [32] N. Novak, R. Pirc, M. Wencka, and Z. Kutnjak, *Phys. Rev. Lett.* **109**, 037601 (2012).
- [33] H. Takenaka, I. Grinberg, and A. M. Rappe, *Phys. Rev. Lett.* **110**, 147602 (2013).
- [34] H. Zong, D. Xue, T. Lookman, and X. Ding, unpublished.
- [35] R. E. Baumer and M. J. Demkowicz, *Phys. Rev. Lett.* **110**, 145502 (2013).
- [36] D. S. Fisher and D. A. Huse, *Phys. Rev. B* **38**, 373 (1988).
- [37] E. Vincent, in: *Lecture Notes in Physics*, Vol. 716, edited by M. Henkel, M. Pleimling, and R. Sanctuary (Springer, Berlin, Heidelberg, 2007), pp. 7–60.
- [38] Ph. Refregier, E. Vincent, J. Hammann, and M. Ocio, *J. Phys. (Paris)* **48**, 1533 (1987).
- [39] P. E. Jonsson, H. Yoshino, and P. Nordblad, *Phys. Rev. Lett.* **89**, 097201 (2002).
- [40] E. V. Colla, L. K. Chao, M. B. Weissman, and D. Viehland, *Phys. Rev. Lett.* **85**, 3033 (2000).
- F. Cracina, A. Franco, D. Piazza, and C. Galassi, *Phys. Rev. Lett.* **93**, 097601 (2004).
- [41] O. Kircher and R. Bohmer, *Eur. Phys. J.* **26**, 329 (2002).